nature biotechnology

Spatially addressed combinatorial protein libraries for recombinant antibody discovery and optimization

Hongyuan Mao[1], James J Graziano[1], Tyson M A Chase[1], Cornelia A Bentley[1], Omar A Bazirgan[1], Neil P Reddy[1], Byeong Doo Song[1,3] & Vaughn V Smider[1,2]

Antibody discovery typically uses hybridoma- or display-based selection approaches, which lack the advantages of directly screening spatially addressed compound libraries as in small-molecule discovery. Here we apply the latter strategy to antibody discovery, using a library of ~10,000 human germline antibody Fabs created by *de novo* DNA synthesis and automated protein expression and purification. In multiplexed screening assays, we obtained specific hits against seven of nine antigens. Using sequence-activity relationships and iterative mutagenesis, we optimized the binding affinities of two hits to the low nanomolar range. The matured Fabs showed full and partial antagonism activities in cell-based assays. Thus, protein drug leads can be discovered using surprisingly small libraries of proteins with known sequences, questioning the requirement for billions of members in an antibody discovery library. This methodology also provides sequence, expression and specificity information at the first step of the discovery process, and could enable novel antibody discovery in functional screens.

Recombinant antibodies are now a major class of therapeutics with over 20 US Food and Drug Administration (FDA)-approved molecules in use for a myriad of diseases. Currently only two main approaches exist for antibody discovery: (i) animal immunization followed by hybridoma[1] or B-cell isolation[2,3] and (ii) library display technologies. Immunization led to the initial discovery of all currently marketed therapeutic antibodies; however, it is a time consuming process that usually leads to antibodies that require further engineering like humanization and affinity maturation. Molecular display libraries have contributed greatly to antibody discovery and engineering, with high affinity and specificity being generated through numerous mutagenesis and selection techniques[4]. Highly diverse libraries containing antibody V_H and V_L genes linked to their encoded proteins can be produced in a number of formats including phage[5,6], ribosome[7], yeast[8] and mammalian cell[9,10] display systems. Such libraries can often reach complexities of 10^{10}–10^{14}, which allow rare high-affinity binders to be identified through competitive selection on target antigens[4].

Display-based libraries have limitations because they rely on competitive selection based on target affinity[11]. They may miss protein molecules with properties that are often incompatible with high affinity, such as agonists, partial agonists and antagonists, and modulators of target function. Modulating a pathway through 'rheostat'-based therapeutics might be pharmacologically more desirable than turning a pathway 'on' or 'off' with high-affinity binders. Many small molecules with modulatory properties are currently approved drugs and are highly sought after[12]. Another drawback of display-based libraries is that several major pharmacologic target classes (e.g., G protein–coupled receptors and ion channels) are largely refractory to antibody discovery because of either their low expression in cell lines or difficulties in producing properly folded purified proteins for affinity selections.

To enable discovery of novel antibodies without the drawbacks of display systems, we sought to exploit the common key property of other methods for interrogating molecular interactions, such as microarrays[13,14] and combinatorial chemistry libraries[15,16]. Namely, each library member is spatially addressed, wherein each molecule is at a discrete location with a priori knowledge of the contents at each position. This format allows each molecule to be interrogated independently, providing data on every library member simultaneously. Moreover, it provides control of reactant concentrations in biochemical assays, allows multiplexed analysis and is also amenable to functional types of cell-based assays. Thus, at a fundamental level, antibody discovery currently relies on genetic selection mechanisms, which do not offer the advantages of the one-by-one screening approaches used to discover small molecules. Technical challenges and costs, though, make it impractical to express and purify the individual proteins needed to generate a spatially addressed antibody library that contains on the order of 10^8 members, the minimum required size suggested by some empirical and theoretical work[17].

A number of lines of evidence, however, suggest that a spatially addressed library comprising tens of thousands of individual members should be sufficient for successful low-affinity lead discovery. First, the actual diversity of naive B cells capable of responding to antigen at any given time in a mouse is only 10^4, based on experimental data[18] and paratope minimal repertoire theory[19]. Second, transgenic mice with a severely restricted V_H combinatorial repertoire can produce antibodies against most antigens, calling into

[1]Fabrus LLC, La Jolla, California, USA. [2]The Scripps Research Institute, La Jolla, California, USA. [3]Present address: Scripps Korea Antibody Institute, Chuncheon-si, Korea. Correspondence should be addressed to V.V.S. (vvsmider@scripps.edu).

Received 24 June; accepted 27 September; published online 24 October 2010; doi:10.1038/nbt.1694

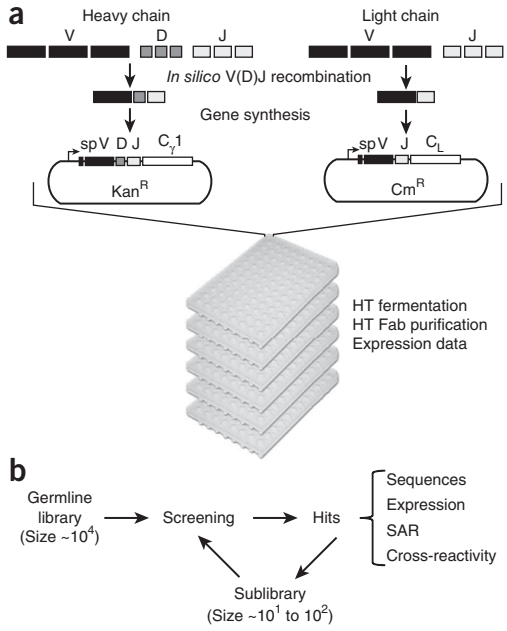

Figure 1 A spatially addressed antibody library for discovery and optimization. (**a**) Schematic of spatially addressed combinatorial library design and generation. (**b**) Schematic of screening and optimization.

question the importance of large numbers of antigen receptors *in vivo*[20]. Third, germline antibodies contain flexible complementarity-determining region (CDR) loops, which gives them the ability to adopt more than one conformation of the antigen binding site[21–26], suggesting that a functional single precursor could respond to more than one antigen[23,25,27,28]. Fourth, as all of the antibody V (variable), D (diversity) and J (joining) gene segments are now known[29], along with the machinery and mechanisms that generate recombinational and junctional diversity[30], it is possible to calculate that all rearranged VDJ heavy chains, when combined with all VJ rearranged light chains, could produce a theoretical repertoire of only ~2×10^7 in the absence of junctional diversity. This number can be further reduced by eliminating redundant amino acid sequences and highly homologous V regions. Although junctional sequence diversification through insertions and deletions can greatly expand the diversity of the repertoire, terminal deoxynucleotidyl transferase (TdT) is not active in the neonatal or B1a B-cell repertoires, and TdT knockout mice show no obvious humoral defects[31]. Furthermore, a protein array screen of >27,000 human proteins against 12 naive antibodies identified four specific interactions[32], suggesting the feasibility of a screening approach with small libraries.

Based on the above considerations, we developed an approach for antibody discovery and optimization using a spatially addressed library of 10^4 lead molecules (**Fig. 1**). Arrayed libraries of highly purified soluble human germline Fabs in microtiter plates were produced using *de novo* DNA synthesis and automated parallel protein expression and purification. Each well contained a unique VDJ recombined heavy chain and VJ recombined light chain, with sequences known a priori. These protein-based libraries are analogous to combinatorial chemistry small-molecule libraries. A high-throughput binding assay using multiplex electrochemiluminescence (ECL) was developed, and antibodies with micromolar binding affinity were identified for several targets. Two hits were further affinity matured. Using the sequence-activity-relationship (SAR) information from adjacent sequence space of either the heavy chain or light chain, we quickly identified important binding regions on the Fabs. This information provided guidance for further optimization toward higher binding affinity. The matured antibodies had both partial and full antagonist activities. We validated the function of these affinity matured antibodies in cell-based assays. Hence, we have demonstrated that a small-molecule discovery paradigm can be applied to large-molecule protein therapeutics, opening up new opportunities in biologic discovery.

RESULTS

Library generation

Our goal was to design a library with the highest structural diversity in a relatively small number of Fabs that could be screened in a spatially addressed format. Initially, all human germline V, D and J sequences were gathered. We chose to omit redundant V-region sequences (>90% homology) and also restricted the D-region sequence reading frames to those encoding the most hydrophilic sequences, which are favored *in vivo*[33]. All V(D)J recombinations were then generated *in silico* (without nucleotide insertions or deletions) resulting in a database of 3,022,272 (7,128 heavy chains × 424 light chains) sequences. A reverse BLAST algorithm was applied in an effort to assess the diversity of all recombined sequences. Following this, 353 of the most diverse sequences were chosen for the heavy chain and 60 for the light chain, creating a library of 21,120 possible Fab sequences. In this scheme, a diverse structural repertoire was anticipated because most framework regions were used. A more focused subset was also created where the commonly used V_H3-23 region[34] was recombined with all possible D and J segments. Thus, the complete germline VDJ diversity of 690 recombinants was sampled for this single heavy-chain framework.

We created a Fab library by the scalable combinatorial association of separate heavy and light chain genes (**Fig. 1a**). Plasmid vectors containing compatible replication origins[35] were designed to facilitate the separate cloning of variable regions of heavy or light chains (V_H and V_L) in frame with the appropriate constant regions[36]. With ~1,000 heavy chain clones and 60 light chain clones, we could theoretically create a Fab library size of 60,000. In practice, typically 96 heavy-chain genes were individually co-transformed with a single light-chain gene. This was done in parallel with six light-chain genes per iteration. Co-transformed cultures (6 × 96-well plates) served as the inocula for a production run in the Piccolo automated protein expression and purification system[37] followed by a secondary purification on protein G running in parallel. Each cycle took ~7 d and theoretically would result in 576 unique highly purified Fabs. However, ~10% were very low expressers with yields ranging from several micrograms to ~400 μg per sample, largely depending on the heavy- and light-chain sequence composition (**Supplementary Figs. 1** and **2**).

Library screening and hit identification

As the number of germline Fabs in our library accumulated into the thousands, we designed a screening assay platform meeting several predefined criteria. We required that the assay: (i) be robust enough to detect weak binders with micromolar range affinities, (ii) be amenable to multiplex analysis to provide binding information on several targets of interest simultaneously and (iii) use low volumes to minimize the consumption of the library. Toward these goals, we developed a binding assay using Meso Scale Discovery's multiplex ECL platform, where each well of a 96-well plate contains nine targets and one blank (**Fig. 2a**). The screening was carried out in a homogenous binding environment, where Fab and a ruthenium-labeled secondary

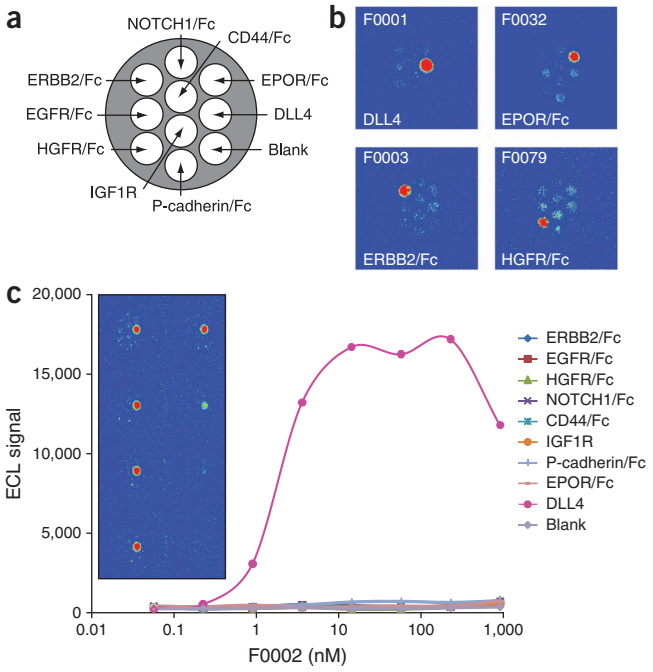

Figure 2 Screening and identifying hits using ECL detection. (**a**) Antigen map of the ten-spot 96-well plate used in the screen. (**b**) Examples of four hits identified from ECL detection: F0001 against DLL4, F0003 against ERBB2/Fc, F0032 against EPOR/Fc and F0079 against HGFR/Fc. Quantified ECL signals are listed in **Supplementary Table 1**. (**c**) Titration of F0002 confirms its binding affinity and specificity to DLL4. Serial dilutions of F0002 were tested (ECL image is inset), and the resulting signal for each of the ten spots is graphed as a function of F0002 concentration.

antibody were both present (without any washing steps). ECL signal was produced only upon Fab binding to a target antigen. We defined a hit as being fourfold above the electrochemiluminescence signal of the blank spot in the same well, with a specific signal defined by binding to only one or two antigens. **Figure 2b** shows ECL image outputs for several specific hits with signal to only one antigen (quantified ECL data are in **Supplementary Table 1**). Polyspecific binding Fabs could also be identified (**Supplementary Fig. 3**). A follow-up titration (**Fig. 2c** and **Supplementary Table 2**) verified the hits and provided information on relative binding strength.

Screening 10,024 Fabs[38] using this method revealed 85 hits against seven of nine antigens. The number of specific hits ranged from four against P-cadherin, to 30 against the erythropoietin receptor (EPOR) (**Supplementary Table 3**). We measured the affinity (K_d) of seven of these hits and found them to be generally in the micromolar range as measured by surface plasmon resonance (SPR). The values from highest affinity to lowest were 500 nM (P-cadherin), 730 nM (DLL4), 4.8 μM (DLL4), 5.6 μM (EPOR), 8.3 μM (EPOR), 38 μM (DLL4) and 65 μM (ERBB2). These data are consistent with our expectation of identifying low-affinity germline Fabs. Sequence information for the hits revealed that some hits against the same target were derived from similar V, D or J sequences. In other circumstances, disparate V, D or J sequences were identified in Fab hits against the same target. For example, among the hits identified for EPOR binding, we observed four V_H sequences (V_H1-46, V_H4-28, V_H4-31 and V_H3-23) and ten V_L sequences (B3, L2, A17, A27, L12, O1, O12, L6, V2-6 and V2-17).

Identification of hits against DLL4

One of our target antigens was human delta-like ligand 4 (DLL4), an important ligand in the NOTCH signaling pathway[39]. DLL4 is a transmembrane protein that is restricted largely to the endothelium of developing vessels and to a small number of additional tissues, such as the thymus, retina, brain, neural tube and hematopoietic cells[39,40]. Upregulation of DLL4 expression in endothelial vessels in adult humans has been observed in a variety of solid tumors[41–43]. Inhibition of the DLL4-NOTCH1 interaction has shown antitumor and anti-cancer stem cell effects in animal models[44–46], presumably by promoting excessive nonproductive neovascularization in the tumor. High-affinity antagonist antibodies targeting DLL4 are now in clinical trials, however, their safety has been questioned owing to hepatic toxicity with repeated use[47]. Thus, alternative activities in targeting DLL4 could be clinically relevant.

Upon screening the library, we identified 18 hits against human DLL4. The V_H and V_L compositions of these hits cover several different families, suggesting diverse DLL4 binding epitopes. The binding constants (K_d) of four Fabs ranged from 0.5 μM (F0030) to 38 μM (F0003) using SPR. Two Fabs (F0001, 4.8 μM; and F0002, 0.73 μM) were chosen for further affinity maturation because they have completely different V_H and V_L sequences—one with a λ-light chain, the other with a κ-light chain, respectively.

Affinity maturation

To avoid creating a large mutagenesis library and to avoid applying display-based selection, we developed a systematic process to optimize the low-affinity binders identified from the germline library. In our spatially addressed format, we can compare binding affinities of the hit versus nearby non-hit Fabs in sequence space because their sequence identities are known a priori. Such comparisons can reveal SARs of important CDR(s) and potentially important residues within the CDRs for binding the target.

In the case of F0002, a closely related non-hit Fab was first identified (**Fig. 3a**). Both Fabs have the same light chain and share the same heavy chain V segment. Only six amino acids in the heavy chain CDR3 are different, accounting for their differences in binding to DLL4. We applied alanine-scanning mutagenesis within the CDR3 and observed that substitution of E100, Y101, S105, E107 or Q110 caused a reduction in DLL4 binding, whereas mutation of S102, S103, S104 or H111 either improved or did not affect binding affinity to DLL4 (**Supplementary Table 4**). Because these latter four are adjacent to residues important for binding, we concluded that these wild-type residues may not be optimal and should be further substituted with other amino acids. From a mutant library, we identified that the S102A (M0007), S103P (M0006), S104F (M0003) and H111F single mutations each enhanced DLL4 binding (**Table 1**). The combined S102A, S103P and S104F triple mutant (M0008) led to sixfold improvement in affinity, and addition of H111F as a quadruple mutant (M0010) conferred a tenfold improvement compared to the parent F0002 (**Table 1** and **Fig. 3b**,**c**). By applying the same mutation principles sequentially, we identified four additional mutants (I51V, N52L, S54T and G56H) in the heavy-chain CDR2, three mutants (S28N, S30D and S31H) in CDR1 and two mutants (S52L and A55S) in CDR2 of the light chain that contribute to binding improvements (**Table 1** and **Fig. 3b**,**c**). By combining all these mutations we effectively matured the DLL4 binding affinity from 730 nM (F0002) to 1.7 nM (M0026), a 430-fold enhancement (**Table 1** and **Fig. 3b**,**c**).

We also applied similar SAR-guided, affinity-maturation principles to the germline hit F0001. By combining five mutations (G24T, S28R, G35V, G100K and G104T) in the heavy chain and three mutations

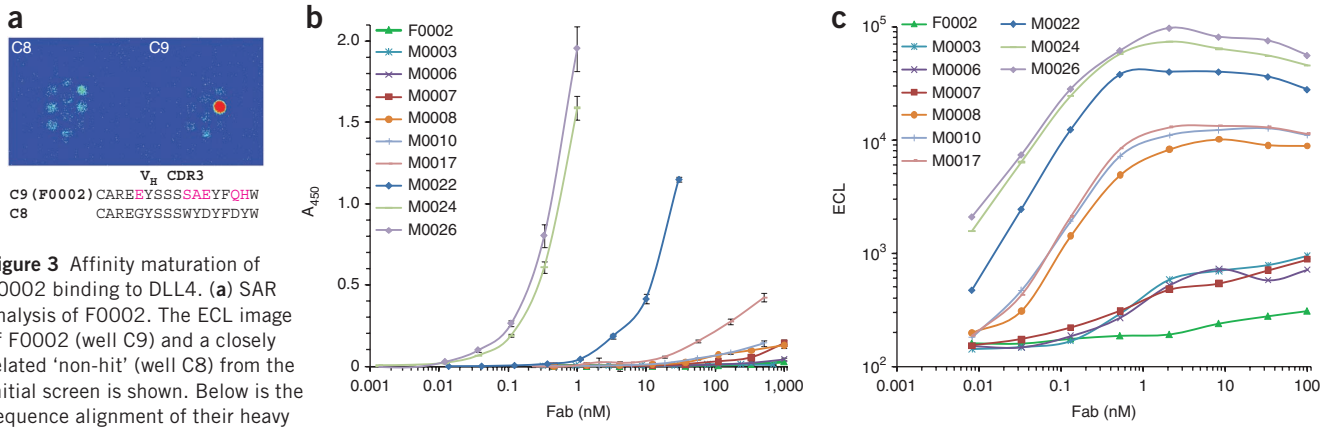

Figure 3 Affinity maturation of F0002 binding to DLL4. (**a**) SAR analysis of F0002. The ECL image of F0002 (well C9) and a closely related 'non-hit' (well C8) from the initial screen is shown. Below is the sequence alignment of their heavy chain CDR3s (residues 96 to 112). Both Fabs share the same light chain and a similar heavy chain, the only differences are six amino acids within the CDR3 of their heavy chains. (**b**) ELISA titration of F0002 and its affinity-matured mutants binding to DLL4. Error bars, s.d. ($n = 3$). (**c**). ECL titration of F0002 and affinity-matured mutants binding to DLL4.

(S52G, V91L and S96P) in the light chain, we effectively matured the DLL4 binding affinity from 4,800 nM (F0001) to 3 and 5 nM (M0034 and M0035), a 1,000-fold improvement (**Table 1**). During affinity maturation of both F0001 and F0002, the specificity toward DLL4 was confirmed by our multiplex binding analysis. Thus, SARs and directed mutations in the absence of competitive selection can guide protein affinity maturation in a manner analogous to the optimization of small-molecule hits using medicinal chemistry.

Epitope mapping of the anti-DLL4 antibodies

The divergent sequences of F0001 and F0002 suggest they might bind different epitopes. To test this hypothesis, we designed an ECL-based competition assay. Ru-labeled M0008, derived from F0002, served as the detection reagent. We chose unlabeled M0022 and M0031 (**Table 1**), which have similar affinities to DLL4 (K_ds = 32.7 ± 11.6, 36.2 ± 8.5 nM, respectively), as competitors in an equilibrium competition assay. M0022 and M0008 are affinity matured mutants from F0002, and should bind to the same epitope on DLL4; whereas M0031, derived from F0001, uses completely different heavy and light chain genes. **Figure 4a** shows that at equilibrium M0022 competes efficiently with M0008 for binding on DLL4, with a competition K_d of about 30 nM. In contrast, M0031 shows much weaker competition. At 400 nM M0031, only 33% of Ru-labeled M0008 was competed. This result confirmed that M0022 and M0031 have either minimally overlapping or different epitopes on DLL4.

To identify the exact binding location on DLL4, a series of recombinant DLL4 extracellular domain truncations (**Fig. 4b**) with C-terminal myc and His tags were made in Chinese hamster ovary (CHO) cells. The expression and relative sizes of these proteins were confirmed by a western blot probed with anti-myc antibody

Table 1 Affinity-maturation mutations in F0002 and F0001 and their corresponding binding affinities to DLL4

	Residues															
	H2	H2	H2	H2	H3	H3	H3	H3	L1	L1	L1	L2	L2	k_{on} ($\times 10^5$), $M^{-1}s^{-1}$	k_{off} ($\times 10^{-3}$), s^{-1}	K_d nM
Fab	51	52	54	56	102	103	104	111	28	30	31	52	55			
F0002	**I**	**N**	**S**	**G**	**S**	**S**	**S**	**H**	**S**	**S**	**S**	**S**	**A**	1.63	101	730
M0003							F							5.00	190	380
M0006						P								–	–	–
M0007					A									–	–	–
M0008					A	P	F							4.05	49.2	121.5
M0010					A	P	F	F						4.25	30.0	70.6
M0017					A	P	F	F	N	D	H			4.44	68.9	155.2[a]
M0022				H	A	P	F	F						3.51	10.1	32.7
M0024	V	L	T	H	A	P	F	F	N	D	H			4.30	1.1	2.7
M0026	V	L	T	H	A	P	F	F	N	D	H	L	S	6.84	1.2	1.7

	Residues											
			H2	H2	H2	H3	H3	L2	L3	L3	k_{on} ($\times 10^5$), $M^{-1}s^{-1}$	k_{off} ($\times 10^{-3}$), s^{-1}	K_d nM
Fab			24	28	35	100	104	52	91	96			
F0001			**G**	**S**	**G**	**G**	**G**	**S**	**V**	**S**			4,800
M0001						K					–	–	–
M0005							T				–	–	–
M0009						K	T				0.6	23	355
M0029				R		K	T				7.4	84.5	114
M0031			T	R	V	K	T				20.9	71.7	36.2
M0034			T	R	V	K	T		L	P	110	36	3.3
M0035			T	R	V	K	T	G	L	P	29.6	14.7	5.0

The binding constants are determined by SPR using Bio-Rad ProteOn XPR36.
[a]M0017 displayed two-site binding: 89% with K_d of 155.2 nM and 10% with 14 nM.

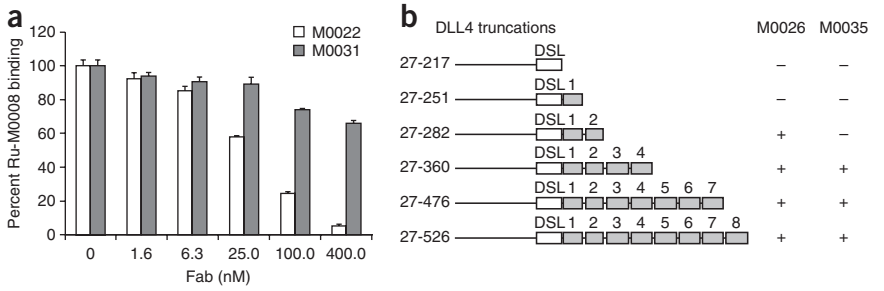

Figure 4 Epitope mapping the anti-DLL4 Fabs binding sites on the DLL4 extracellular domain. (**a**) ECL-based competition binding assay. Competition between the binding of Ru-labeled M0008 and increased concentrations of either unlabeled M0022 or M0031 to DLL4, quantified by ECL. Error bars, s.d. ($n = 2$). (**b**) Mapping of DLL4 binding region of M0026 and M0035 using an unreduced western blot. A series of DLL4 extracellular domain truncations are depicted in the cartoon diagram, where the DSL domain is highlighted as the open rectangular box; and the EGF-like domains 1 to 8 are highlighted as the shaded rectangular boxes labeled as 1, 2, etc. Anti-DLL4 binding observed in the westerns is marked as +, and no binding is marked as –.

(data not shown). M0026 (derived from F0002) binding involves the EGF2 domain (amino acid (aa) 252 to 286), and M0035 (derived from F0001) binds between EGF2 to EGF4 domains (aa 252 to 360) (**Fig. 4b**). Both anti-DLL4 Fabs appear to recognize conformational epitopes formed in the presence of disulfide bonds because their binding was abolished when the DLL4 protein was first treated with a reducing reagent.

Functional activity of affinity-matured Fabs

We next sought to evaluate the biological function of the affinity-matured Fabs in the context of the NOTCH1-DLL4 interaction in cell-based assays. First, the binding of M0026 and M0035 to DLL4 overexpressed on the surface of CHO cells (CHO-DLL4) was confirmed using phycoerythrin-labeled secondary antibody (**Fig. 5a**,**b**). Biotinylated NOTCH1-Fc binding to CHO-DLL4 was also confirmed using streptavidin-phycoerythrin as the detection reagent (**Fig. 5c**). Neither Fab showed significant binding to CHO cells without DLL4 overexpression (data not shown). Next, we evaluated whether the DLL4-binding Fabs could compete with NOTCH1-Fc binding to CHO-DLL4. Biotinylated NOTCH1-Fc was incubated with CHO-DLL4 in the presence of different concentrations of unlabeled M0026 or M0035. We confirmed that both anti-DLL4 Fabs could effectively block NOTCH1-Fc binding to CHO-DLL4 (**Fig. 5d**). Specifically, 2 nM M0026 or 50 nM M0035 competed for more than 80% of NOTCH1 binding activity, with M0026 showing stronger competition than M0035.

We next asked whether M0026 and M0035 could inhibit DLL4-dependent NOTCH1 signaling using a luciferase reporter assay. Human glioma T98G cells[48], known for the presence of NOTCH1 on their cell surface, were stably transfected with a NOTCH1 reporter plasmid (p6 × CBF) containing six C promoter binding factor-1 (CBF-1) response elements[49]. Firefly luciferase expression was driven through the NOTCH1-DLL4 interaction upon cell contact by addition of CHO-DLL4 cells in *trans* to T98G reporter cells. Incubation of the T98G reporter cells with CHO-DLL4 and an irrelevant Fab resulted in eight- to ninefold increase in NOTCH1 reporter levels compared to those incubated with an irrelevant Fab and CHO cells (**Fig. 5e**, compare close triangles to open triangles). The NOTCH1 activation remained constant in the presence of increasing concentrations of the non-DLL4 binding Fab F1001 (**Fig. 5e**). The activation was reduced, however, in the presence of increasing concentrations of anti-DLL4 Fabs M0026 and M0035 (**Fig. 5e**). The reduction was even more pronounced with an IgG version of M0026 (IC_{50} ~6 nM) (**Fig. 5e**), which was almost tenfold more efficient than M0026 Fab. The IgG version of M0035 is also more effective than M0035 Fab, displaying about 30% reduction in NOTCH1 activation at 0.8 nM. However, it did not show complete suppression of NOTCH1 activation at higher concentrations. Clearly, the M0026 IgG is a more potent inhibitor of DLL4-NOTCH1 interaction than M0035 IgG, but only at higher concentrations. Interestingly, M0035 shows partial antagonist activity, being unable to fully inhibit NOTCH1 signaling. Based on these studies, we have demonstrated that target-specific Fabs can be identified from a small germline

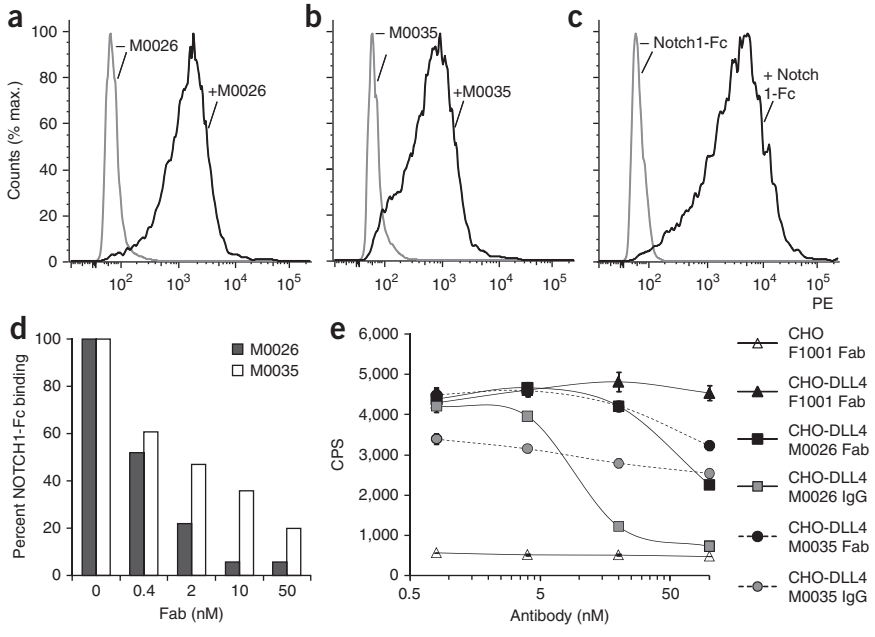

Figure 5 Assays of anti-DLL4 antibodies in cell-based assays. (**a**–**c**) FACS profiles of M0026, M0035 Fabs and NOTCH1-Fc binding to CHO-DLL4 cells. M0026 and M0035 binding was detected using phycoerythrin-labeled anti-human kappa IgGs (PE-α-kappa), phycoerythrin-labeled anti-human lambda IgG (PE-α-lambda), respectively. Biotinylated NOTCH1-Fc binding to CHO-DLL4 was detected with phycoerythrin-labeled streptavidin (PE-strep). (**d**) Anti-DLL4 Fab competition of NOTCH1/Fc binding to CHO-DLL4 cells using FACS. (**e**) Inhibition of NOTCH1 luciferase reporter by anti-DLL4 antibodies. CHO-DLL4 activation of NOTCH1 reporter in T98G cells is inhibited by both M0026 and M0035 Fabs and IgGs in a dose-dependent manner. A control nonbinding Fab (F1001) has no effect on NOTCH1 reporter levels. Shown is background-subtracted counts per second (CPS) with error bars, s. e. ($n = 4$).

repertoire, these Fabs can be engineered to high-affinity, biologically active molecules and unique activities like partial antagonism can be identified.

DISCUSSION

Although monoclonal antibody discovery dates back 35 years, nearly all FDA approved antibodies are high-affinity antagonists and bind soluble proteins or membrane targets with large extracellular domains. All of these antibodies were discovered using methods relying on biological selection. The ability to discover antibodies with novel mechanisms of action or to derive antibodies against more difficult transmembrane targets, or even unknown targets, could benefit from unique discovery systems that obviate affinity-based competitive selection. Direct screening of collections of individually purified germline antibodies could provide these features.

The feasibility of using arrayed protein libraries for drug discovery has not yet been demonstrated for several reasons. First, the number of library members (paratopes) required to ensure the identification of 'hits' against most targets is unknown. Experience with display libraries suggests this number may be ~10^8. For example, nonimmune phage libraries of 3×10^7– 3×10^8 could select binders in the 0.1–2.5 μM K_d range[50–52], whereas libraries of 10^{10} could select binders in the 0.2–70 nM range[53–55]. The immune system, however, can clearly use a much smaller number of naive antibodies (10^4) as the pool capable of responding to any antigen. Second, the technology to produce large numbers of purified proteins at high yield in parallel was not available until the advent of several high-throughput protein crystallography programs (structural genomics projects)[56,57]. Third, the cost of DNA synthesis was prohibitive to constructing such large libraries on a one-by-one basis until recently.

The biochemical properties inherent in screening the spatially addressed library reported here are substantially different than in display-based discovery. First, screening is done at high Fab concentrations. Thus, binding can be driven by greater Fab/target ratios in a spatially addressed format using soluble proteins. In contrast, individual members of a display-based library may only be present at attomolar concentrations or less, which could decrease the likelihood of any given binder from interacting with the target, and necessitate larger display-based library sizes. Second, our screening is accomplished in a homogenous binding situation, in the absence of washing events that can remove binders with fast off-rates and further decrease the concentration of the molecule being screened. Third, our discovery method relies on screening as opposed to selection, thus both low- and high-affinity leads can be identified because they are analyzed in separate wells. In this regard, the sensitivity of detection allows identification of specific hits in the 0.5–50 μM range. The ability to detect very low affinity leads may allow for substantially smaller library sizes to be screened successfully. Fourth, germline antibodies are known to adopt many different conformations, with the ability of a single antibody to bind unrelated antigens due to alternative conformations of flexible CDR loops[21–26,58]. Thus, the actual structural diversity in a library of 10^4 germline antibodies might be significantly higher. In this regard, it has been suggested that the amino acid sequences of V_H CDR3 (encoded largely by the D region) in germline antibodies has been optimized by evolution for maximum flexibility[21]. A small but optimized library for these characteristics might be more efficient at producing binders than other much larger libraries that were generated using *in vivo* affinity-matured V-regions. Lastly, there has been a considerable discrepancy between the apparent library sizes required for discovery of binding proteins using display-based approaches and the actual repertoire size in a mammal that responds to antigen[18]. Because of the selection requirement, and associated washing steps, larger library sizes may be required for display-based discovery. In contrast, we have made a spatially addressed library of a size that is in line with the actual diversity that responds to antigens *in vivo*.

The ability of naive B cells to respond to antigens with a low affinity, followed by subsequent affinity maturation, may allow a small initial repertoire to respond to a multitude of antigens. The ability to achieve robust discovery with such small library sizes in a spatially addressed format could open unique opportunities for biologic discovery of alternative mechanisms of action, novel epitopes, difficult targets, multiplexed screening, multispecific binders or direct screening for functional activity in cell-based assays. Such library sizes (e.g., 10^4) are also well within the limits of most high-throughput discovery efforts using microtiter plates, which make the aforementioned possibilities testable using existing technology. Furthermore, because the sequences are spatially addressed and known a priori, the need to deconvolute the identity of a 'hit' candidate from a single pool of diverse molecules is removed.

A spatially addressed library coupled with the combinatorial nature of V(D)J diversity generation also facilitates identifying SARs that aid in the optimization of preliminary hits, mimicking the approach used in small-molecule medicinal chemistry. Preliminary hits are used to generate an affinity-matured antibody, which contains one or more amino acid alterations that result in an improvement in antigen binding affinity. Currently many of the *in vitro* affinity matured antibodies are produced either by V_H and V_L domain shuffling[52] or by random mutagenesis of CDR and/or framework residues[59–64]. However, many of these methods require some type of displayed selection because of the vast number of clones to be evaluated. In contrast, we adopted a more rational and targeted mutagenesis approach, using much smaller libraries guided by SARs and alanine-scanning mutagenesis to identify regions and residues that modulated affinity. Our antibody discovery method can give true SARs because active hits can be compared with related, but inactive, Fabs present in the library. Only residues with alanine substitutions that were in contact-making CDRs but that did not affect binding (or even conferred improvement) were further mutated individually to other amino acids. We also avoided simultaneous mutations to circumvent exponential expansion of the library size. For a given CDR, once the best substitution was identified in each of the mutated positions, they were combined in the new Fab and were found to provide additive improvement in binding affinity. The increase in affinity, measured as a decrease in K_d, can be achieved through either an increase in association rate (k_{on}), a reduction in dissociation rate (k_{off}), or both. Through the homogenous ECL-screening platform, we were able to capture improvements in both directions.

We used *de novo* DNA synthesis and automated parallel fermentation and purification to generate our arrayed library. The time and costs of library construction are greater than generation of 'one pot' libraries used in display approaches. Compared with small-molecule libraries, however, the standardized production and purification techniques in antibody generation allow the costs to be several orders of magnitude below typical combinatorial chemistry collections. These costs and production efficiencies can likely be further optimized through strain development, alternative hosts, enhanced parallel fermentation conditions, optimized automation engineering or even alternative scaffolds to antibodies[65,66], as well as the continued decrease in the cost of DNA synthesis. Smaller scale production in 96-well blocks could be accomplished routinely in most molecular biology laboratories using standard strains and micropurification techniques. Furthermore, the discovery efficiency could potentially

be improved by increasing the library size, presenting the antigen in an ordered manner on the solid surface or through miniaturization methods to allow more targets to be screened in smaller volumes[3].

Small-molecule drugs have several mechanisms of action, including acting as antagonists, agonists, partial agonists or antagonists and modulators. In contrast, most currently marketed antibodies act as antagonists. The discovery selection mechanisms in hybridoma and display-based systems, which drive affinity and dominant epitope binding, could be reasons for this bias. There is no inherent biochemical reason why antibodies cannot act by alternative mechanisms of action like small-molecule drugs. The M0035 Fab and IgG has partial antagonist activity, and has a qualitatively different activity compared to M0026, which has a similar affinity but binds a different epitope. Discovery of functional activities beyond high-affinity antagonism is a potentially fruitful and largely unexplored area for monoclonal antibody therapeutics. Indeed, unique functional antibodies have been disclosed in a few reports[67]. A limited number of agonist antibodies have been described[68] and some are now in clinical development[69]. The ability to reproducibly identify such antibodies will require unique discovery systems. The spatially addressed library reported here could enable direct identification of more unique antibodies with novel mechanisms of action beyond antagonism.

METHODS

Methods and any associated references are available in the online version of the paper at http://www.nature.com/naturebiotechnology/.

Note: Supplementary information is available on the Nature Biotechnology website.

ACKNOWLEDGMENTS

We thank D. Myszka from Biosensor Tools for measuring binding affinities of our Fabs using surface plasmon resonance, R. Lerner for comments on the manuscript, P. Schultz and W. Huse for useful discussions and M. Sandburg and Y. Jiang from Wintherix for their help with the FACS instrument.

AUTHOR CONTRIBUTIONS

H.M. designed and constructed the plasmid vectors for heavy and light chain library; performed Fab library generation; designed and executed affinity maturations, including alanine-scanning mutagenesis, NNK mutagenesis and cassette mutagenesis, of F0001 and F0002; performed a small subset of library screening using ECL; conducted ECL based epitope mapping competition assay. H.M. also designed the cloning strategy for constructing the V_H3-23 library with all possible germline D-J combinations, together with T.M.A.C., J.J.G., C.A.B., O.A.B. and N.P.R. made the V_H3-23 library. J.J.G. performed the automated expression and purification on Piccolo. J.J.G. and V.V.S. designed the software for generating the V(D)J recombinant sequences and selecting the representative sequences for gene synthesis. T.M.A.C. performed the majority of the library screening using ECL and performed ELISA on the affinity matured Fabs with DLL4. C.A.B. performed the Fab binding assays on CHO-DLL4 cells using FACS and executed inhibition assays of NOTCH1-DLL4 interaction using ELISA and FACS. C.A.B. and O.A.B. designed and performed the Luciferase reporter assays on inhibition of NOTCH1-DLL4 interaction. N.P.R. made all DLL4 extracellular domain constructs and executed the epitope mapping with western blots, generated CHO-DLL4 cell line and helped H.M. for Fab library transformation. B.D.S. also supervised the construction of DLL4 extracellular domains. O.A.B. made the NOTCH1 reporter plasmid (p6xCBF), which was modified from an earlier reporter plasmid (p4XCBF) made by B.D.S. O.A.B. also constructed the full length IgG eukaryotic expression vectors and expressed and purified the IgGs. V.V.S. conceptualized the spatially addressed antibody library and oversaw the concept development at Fabrus. V.V.S. and H.M. wrote the manuscript. All authors discussed and commented on the manuscript.

COMPETING FINANCIAL INTERESTS

The authors declare competing financial interests: details accompany the full-text HTML version of the paper at http://www.nature.com/naturebiotechnology/.

Published online at http://www.nature.com/naturebiotechnology/.
Reprints and permissions information is available online at http://npg.nature.com/reprintsandpermissions/.

1. Kohler, G. & Milstein, C. Continuous cultures of fused cells secreting antibody of predefined specificity. *Nature* **256**, 495–497 (1975).
2. Jin, A. *et al.* A rapid and efficient single-cell manipulation method for screening antigen-specific antibody-secreting cells from human peripheral blood. *Nat. Med.* **15**, 1088–1092 (2009).
3. Love, J.C., Ronan, J.L., Grotenbreg, G.M., van der Veen, A.G. & Ploegh, H.L. A microengraving method for rapid selection of single cells producing antigen-specific antibodies. *Nat. Biotechnol.* **24**, 703–707 (2006).
4. Hoogenboom, H.R. Selecting and screening recombinant antibody libraries. *Nat. Biotechnol.* **23**, 1105–1116 (2005).
5. Huse, W.D. *et al.* Generation of a large combinatorial library of the immunoglobulin repertoire in phage lambda. *Science* **246**, 1275–1281 (1989).
6. McCafferty, J., Griffiths, A.D., Winter, G. & Chiswell, D.J. Phage antibodies: filamentous phage displaying antibody variable domains. *Nature* **348**, 552–554 (1990).
7. Hanes, J., Jermutus, L., Weber-Bornhauser, S., Bosshard, H.R. & Pluckthun, A. Ribosome display efficiently selects and evolves high-affinity antibodies in vitro from immune libraries. *Proc. Natl. Acad. Sci. USA* **95**, 14130–14135 (1998).
8. Boder, E.T. & Wittrup, K.D. Yeast surface display for screening combinatorial polypeptide libraries. *Nat. Biotechnol.* **15**, 553–557 (1997).
9. Beerli, R.R. *et al.* Isolation of human monoclonal antibodies by mammalian cell display. *Proc. Natl. Acad. Sci. USA* **105**, 14336–14341 (2008).
10. Ho, M., Nagata, S. & Pastan, I. Isolation of anti-CD22 Fv with high affinity by Fv display on human cells. *Proc. Natl. Acad. Sci. USA* **103**, 9637–9642 (2006).
11. Levitan, B. Stochastic modeling and optimization of phage display. *J. Mol. Biol.* **277**, 893–916 (1998).
12. Wang, L., Martin, B., Brenneman, R., Luttrell, L.M. & Maudsley, S. Allosteric modulators of g protein-coupled receptors: future therapeutics for complex physiological disorders. *J. Pharmacol. Exp. Ther.* **331**, 340–348 (2009).
13. Fodor, S.P. *et al.* Light-directed, spatially addressable parallel chemical synthesis. *Science* **251**, 767–773 (1991).
14. Ziauddin, J. & Sabatini, D.M. Microarrays of cells expressing defined cDNAs. *Nature* **411**, 107–110 (2001).
15. Diller, D.J. The synergy between combinatorial chemistry and high-throughput screening. *Curr. Opin. Drug Discov. Devel.* **11**, 346–355 (2008).
16. Polinsky, A. Combichem and chemoinformatics. *Curr. Opin. Drug Discov. Devel.* **2**, 197–203 (1999).
17. Kauffman, S.A.. *The Origins of Order* (Oxford University Press; 1993).
18. Bachmann, M.F., Kundig, T.M., Kalberer, C.P., Hengartner, H. & Zinkernagel, R.M. How many specific B cells are needed to protect against a virus? *J. Immunol.* **152**, 4235–4241 (1994).
19. Cohn, M. & Langman, R.E. The protection: the unit of humoral immunity selected by evolution. *Immunol. Rev.* **115**, 11–147 (1990).
20. Xu, J.L. & Davis, M.M. Diversity in the CDR3 region of V(H) is sufficient for most antibody specificities. *Immunity* **13**, 37–45 (2000).
21. Babor, M. & Kortemme, T. Multi-constraint computational design suggests that native sequences of germline antibody H3 loops are nearly optimal for conformational flexibility. *Proteins* **75**, 846–858 (2009).
22. Patten, P.A. *et al.* The immunological evolution of catalysis. *Science* **271**, 1086–1091 (1996).
23. Sethi, D.K., Agarwal, A., Manivel, V., Rao, K.V. & Salunke, D.M. Differential epitope positioning within the germline antibody paratope enhances promiscuity in the primary immune response. *Immunity* **24**, 429–438 (2006).
24. Thielges, M.C., Zimmermann, J., Yu, W., Oda, M. & Romesberg, F.E. Exploring the energy landscape of antibody-antigen complexes: protein dynamics, flexibility, and molecular recognition. *Biochemistry* **47**, 7237–7247 (2008).
25. Yin, J., Beuscher, A.E.t., Andryski, S.E., Stevens, R.C. & Schultz, P.G. Structural plasticity and the evolution of antibody affinity and specificity. *J. Mol. Biol.* **330**, 651–656 (2003).
26. Zimmermann, J. *et al.* Antibody evolution constrains conformational heterogeneity by tailoring protein dynamics. *Proc. Natl. Acad. Sci. USA* **103**, 13722–13727 (2006).
27. Nguyen, H.P. *et al.* Germline antibody recognition of distinct carbohydrate epitopes. *Nat. Struct. Biol.* **10**, 1019–1025 (2003).
28. Thomson, C.A. *et al.* Germline V-genes sculpt the binding site of a family of antibodies neutralizing human cytomegalovirus. *EMBO J.* **27**, 2592–2602 (2008).
29. Matsuda, F. *et al.* The complete nucleotide sequence of the human immunoglobulin heavy chain variable region locus. *J. Exp. Med.* **188**, 2151–2162 (1998).
30. Smider, V. & Chu, G. The end-joining reaction in V(D)J recombination. *Semin. Immunol.* **9**, 189–197 (1997).
31. Gilfillan, S., Benoist, C. & Mathis, D. Mice lacking terminal deoxynucleotidyl transferase: adult mice with a fetal antigen receptor repertoire. *Immunol. Rev.* **148**, 201–219 (1995).
32. Holt, L.J., Bussow, K., Walter, G. & Tomlinson, I.M. By-passing selection: direct screening for antibody-antigen interactions using protein arrays. *Nucleic Acids Res.* **28**, E72 (2000).
33. Corbett, S.J., Tomlinson, I.M., Sonnhammer, E.L., Buck, D. & Winter, G. Sequence of the human immunoglobulin diversity (D) segment locus: a systematic analysis provides no evidence for the use of DIR segments, inverted D segments, "minor" D segments or D-D recombination. *J. Mol. Biol.* **270**, 587–597 (1997).
34. Brezinschek, H.P. *et al.* Analysis of the human VH gene repertoire. Differential effects of selection and somatic hypermutation on human peripheral CD5(+)/IgM+ and CD5(–)/IgM+ B cells. *J. Clin. Invest.* **99**, 2488–2501 (1997).

35. Kim, D. *et al.* Directed evolution and identification of control regions of ColE1 plasmid replication origins using only nucleotide deletions. *J. Mol. Biol.* **351**, 763–775 (2005).
36. Leonard, B., Sharma, V. & Smider, V. Co-expression of antibody fab heavy and light chain genes from separate evolved compatible replicons in *E. coli*. *J. Immunol. Methods* **317**, 56–63 (2006).
37. Wollerton, M.C., Wales, R., Bullock, J.A., Hudson, I.R. & Beggs, M. Automation and optimization of protein expression and purification on a novel robotic platform. *JALA* **11**, 291–303 (2006).
38. Smider, V. *et al.* Combinatorial antibody libraries and uses thereof. PCT/US2009/063299 (2009).
39. Shutter, J.R. *et al.* Dll4, a novel Notch ligand expressed in arterial endothelium. *Genes Dev.* **14**, 1313–1318 (2000).
40. Yoneya, T. *et al.* Molecular cloning of delta-4, a new mouse and human Notch ligand. *J. Biochem.* **129**, 27–34 (2001).
41. Li, J.L. *et al.* Delta-like 4 Notch ligand regulates tumor angiogenesis, improves tumor vascular function, and promotes tumor growth in vivo. *Cancer Res.* **67**, 11244–11253 (2007).
42. Mailhos, C. *et al.* Delta4, an endothelial specific notch ligand expressed at sites of physiological and tumor angiogenesis. *Differentiation* **69**, 135–144 (2001).
43. Patel, N.S. *et al.* Up-regulation of endothelial delta-like 4 expression correlates with vessel maturation in bladder cancer. *Clin. Cancer Res.* **12**, 4836–4844 (2006).
44. Hoey, T. *et al.* DLL4 blockade inhibits tumor growth and reduces tumor-initiating cell frequency. *Cell Stem Cell* **5**, 168–177 (2009).
45. Patel, N.S. *et al.* Up-regulation of delta-like 4 ligand in human tumor vasculature and the role of basal expression in endothelial cell function. *Cancer Res.* **65**, 8690–8697 (2005).
46. Segarra, M. *et al.* Dll4 activation of Notch signaling reduces tumor vascularity and inhibits tumor growth. *Blood* **112**, 1904–1911 (2008).
47. Yan, M. *et al.* Chronic DLL4 blockade induces vascular neoplasms. *Nature* **463**, E6–E7 (2010).
48. Nefedova, Y., Cheng, P., Alsina, M., Dalton, W.S. & Gabrilovich, D.I. Involvement of Notch-1 signaling in bone marrow stroma-mediated de novo drug resistance of myeloma and other malignant lymphoid cell lines. *Blood* **103**, 3503–3510 (2004).
49. Purow, B.W. *et al.* Expression of Notch-1 and its ligands, Delta-like-1 and Jagged-1, is critical for glioma cell survival and proliferation. *Cancer Res.* **65**, 2353–2363 (2005).
50. de Kruif, J., Boel, E. & Logtenberg, T. Selection and application of human single chain Fv antibody fragments from a semi-synthetic phage antibody display library with designed CDR3 regions. *J. Mol. Biol.* **248**, 97–105 (1995).
51. Mao, S. *et al.* Phage-display library selection of high-affinity human single-chain antibodies to tumor-associated carbohydrate antigens sialyl Lewisx and Lewisx. *Proc. Natl. Acad. Sci. USA* **96**, 6953–6958 (1999).
52. Marks, J.D. *et al.* By-passing immunization: building high affinity human antibodies by chain shuffling. *Bio/Technology* **10**, 779–783 (1992).
53. Griffiths, A.D. *et al.* Isolation of high affinity human antibodies directly from large synthetic repertoires. *EMBO J.* **13**, 3245–3260 (1994).
54. Sheets, M.D. *et al.* Efficient construction of a large nonimmune phage antibody library: the production of high-affinity human single-chain antibodies to protein antigens. *Proc. Natl. Acad. Sci. USA* **95**, 6157–6162 (1998).
55. Vaughan, T.J. *et al.* Human antibodies with sub-nanomolar affinities isolated from a large non-immunized phage display library. *Nat. Biotechnol.* **14**, 309–314 (1996).
56. Chandonia, J.M. & Brenner, S.E. The impact of structural genomics: expectations and outcomes. *Science* **311**, 347–351 (2006).
57. Joachimiak, A. High-throughput crystallography for structural genomics. *Curr. Opin. Struct. Biol.* **19**, 573–584 (2009).
58. Brooks, C.L. *et al.* Exploration of specificity in germline monoclonal antibody recognition of a range of natural and synthetic epitopes. *J. Mol. Biol.* **377**, 450–468 (2008).
59. Barbas, C.F. III *et al.* In vitro evolution of a neutralizing human antibody to human immunodeficiency virus type 1 to enhance affinity and broaden strain cross-reactivity. *Proc. Natl. Acad. Sci. USA* **91**, 3809–3813 (1994).
60. Cumbers, S.J. *et al.* Generation and iterative affinity maturation of antibodies in vitro using hypermutating B-cell lines. *Nat. Biotechnol.* **20**, 1129–1134 (2002).
61. Hawkins, R.E., Russell, S.J. & Winter, G. Selection of phage antibodies by binding affinity. Mimicking affinity maturation. *J. Mol. Biol.* **226**, 889–896 (1992).
62. Jackson, J.R., Sathe, G., Rosenberg, M. & Sweet, R. In vitro antibody maturation. Improvement of a high affinity, neutralizing antibody against IL-1 beta. *J. Immunol.* **154**, 3310–3319 (1995).
63. Wu, H. *et al.* Stepwise in vitro affinity maturation of Vitaxin, an alphav beta3-specific humanized mAb. *Proc. Natl. Acad. Sci. USA* **95**, 6037–6042 (1998).
64. McCall, A.M. *et al.* Isolation and characterization of an anti-CD16 single-chain Fv fragment and construction of an anti-HER2/neu/anti-CD16 bispecific scFv that triggers CD16-dependent tumor cytolysis. *Mol. Immunol.* **36**, 433–446 (1999).
65. Binz, H.K., Amstutz, P. & Pluckthun, A. Engineering novel binding proteins from nonimmunoglobulin domains. *Nat. Biotechnol.* **23**, 1257–1268 (2005).
66. Skerra, A. Alternative non-antibody scaffolds for molecular recognition. *Curr. Opin. Biotechnol.* **18**, 295–304 (2007).
67. Miller, D.J. & Rodriguez, M. A monoclonal autoantibody that promotes central nervous system remyelination in a model of multiple sclerosis is a natural autoantibody encoded by germline immunoglobulin genes. *J. Immunol.* **154**, 2460–2469 (1995).
68. Liu, Z. *et al.* A potent erythropoietin-mimicking human antibody interacts through a novel binding site. *Blood* **110**, 2408–2413 (2007).
69. Wang, J. *et al.* Characterization of a novel anti-DR5 monoclonal antibody WD1 with the potential to induce tumor cell apoptosis. *Cell. Mol. Immunol.* **5**, 55–60 (2008).

ONLINE METHODS

Library construction. Plasmids A, C and E were constructed to produce the recombinant Fab library. Plasmid A was used for expressing the heavy chains, plasmid C for κ-light chains, and plasmid E for λ light chains. The ColE1-derived replication origins for plasmids A and C (or plasmids A and E) are compatible to each other and replicate at similar copy numbers when co-cultured in the same *Escherichia coli* cell. The plasmids carry a STII leader sequence for Fab secretion and an Ara promoter for inducible gene expression. Plasmid A encodes a C_H region for production of a Fab heavy chain and includes Flag and His tags for protein purification. Plasmid C encodes a C_κ region for production of a κ-Fab light chain while plasmid E encodes a C_λ region for production of a λ-Fab light chain. *In silico* V(D)J recombination of germline antibody gene sequences was performed using proprietary software developed at Fabrus. DNAs encoding the recombined V_H or V_L regions were synthesized by GenScript. The V_H sequences were cloned between the NheI and NcoI sites of plasmid A. The V_κ sequences were cloned between the NcoI and BsiWI of plasmid C, and the V_λ sequence was cloned between the NcoI and AvrII sites of plasmid E using standard molecular biology techniques.

A Fab is produced in *E. coli* upon co-transformation and induction of a plasmid encoding a heavy chain and a plasmid encoding a light chain. Specifically, 1 ng heavy and light chain plasmids were combined in a PCR tube or a PCR 96-tube plate and were mixed well with 20 µl ice cold LMG194 (ATCC)-competent cells. After heat-shock transformation and recovery at 37 °C, the co-transformed cells were selected by growing in 1 ml Luria-Bertani broth containing 0.4% (wt/vol) glucose (Sigma Aldrich), 50 µg/ml kanamycin (Sigma Aldrich) and 34 µg/ml chloramphenicol (Sigma Aldrich) at 32 °C with vigorous shaking for 20 h. To create a Fab genetic library, different heavy chains in 96-well format are co-transformed with multiple light chains in parallel. Sequences of all Fabs in the library are available in ref. 38.

Automated expression and purification. Overnight co-transformation cultures in 96-deep well format were used as inocula for Piccolo instrument (The Automation Partnership) expression and purification of the Fabs[37]. All Piccolo labware was barcoded for tracking through the process. Five liters of sterile Terrific Broth (TB) media was prepared with kanamycin (50 µg/ml), chloramphenicol (35 µg/ml), glucose (2% wt/vol) and antifoam 204 (0.015% vol/vol) (Sigma). Arabinose inducer (0.2% wt/vol) (Sigma) and the prepared media were attached to sterile dispensing pumps. Culture vessel blocks (CVBs) were filled (9.5 ml of media) and inoculated (100 µl per well). After all CVBs were inoculated they were transferred one-by-one to an incubator and growth was monitored by an OD_{600} reading. Upon completion, a CVB was removed from the incubator and 2.5 ml lysis buffer (50 mM sodium phosphate pH 8.0, 300 mM NaCl, 3.25% wt/vol *N*-octyl-β-D thioglucoside (Alexis Biochemicals) and 1:500 dilution of Lysonase (EMD)) was added to each well. Lysis proceeded for 30 min and then the CVB was centrifuged for 30 min at 5,000*g* to pellet the cellular debris. The supernatant was transferred to a filter plate containing 1 ml His-Bind resin (EMD) per well. The resin was then washed 2× with 6 ml of 50 mM sodium phosphate pH 8.0, 300 mM NaCl, 30 mM imidazole and eluted 4× with 500 µl of 50 mM sodium phosphate pH 8.0, 300 mM NaCl, 500 mM imidazole.

Fabs eluted from the His-Bind resin on Piccolo were further purified using a secondary off-line purification step. Depending on the light chain classes, two different affinity resins were applied: Fabs with κ-light chain were further purified on Protein G column (GE Healthcare), and those with λ-light chain were purified on CaptureSelect Fab Lambda affinity column (BAC). Approximately 1.8 ml of the His-Bind elution per Fab sample was purified on either a 1 ml HiTrap Protein G column or a 0.5 ml CaptureSelect Fab Lambda affinity column at 4 °C using the Akta purifier (GE Healthcare) and A-905 autosampler (GE Healthcare) according to the manufacturer's protocol. After four 450 µl injections, the column was washed with two column volumes of 50 mM sodium phosphate pH 7.2, 150 mM NaCl. The Fab was eluted with six column volumes of 100 mM glycine (EMD), pH 2.8. Approximately 0.8 ml of elution peak fractions were collected in a deep well, 96-well plate block, and immediately neutralized with 100 µl saturated dibasic sodium phosphate pH 9.0. The Fab concentration was determined from A_{280} absorbance on a plate reader (Molecular Devices).

Fab library screening. Nine recombinant human antigens (carrier free) were purchased from R&D systems: ERBB2/Fc, EGFR/Fc, HGFR/Fc, NOTCH1/Fc, CD44/Fc, IGF1R, P-cadherin/Fc, EPOR/Fc and DLL4. These antigens were spotted onto 96-well Multi-Spot 10 Highbind plates by Meso Scale Discovery (MSD). Spots 1 to 9 contain 50 nl of 60 µg/ml of antigen each, and spot 10 is left blank. Goat anti-human κ-light chain polyclonal antibody (Sigma Aldrich) and Goat anti-human λ light chain polyclonal antibody (Sigma Aldrich) were conjugated with Ru tri-bispyridine-(4-methysulfone) TAG (MSD) according to the manufacturer's suggested procedures.

The antigen-coated, 96-well Multi-Spot 10 Highbind plate was first blocked with 150 µl of 3% bovine serum albumin (BSA) in Tris-buffered saline containing 0.1% Tween-20 (TBST) per well at 20 °C for 30 min. After washing, 12.5 µl 1% BSA TBST and 12.5 µl of Fab from the purified library were added per well and incubated at 20 °C with shaking for 1 h. Ru-labeled detection antibody (1 µg/ml) was added in 25 µl and incubated at 20 °C with shaking for 1 h. Finally 15 µl of Buffer P with surfactant (MSD) was added to the complex mixture and the plate was read on a Sector Imager 2400 (MSD). The ECL signals of the antigen and the blank in each well were compared and a signal/blank ratio of 4:1 or greater was considered a potential hit. To confirm a potential hit from the initial ECL screening, a secondary titration with sequential dilution was carried out.

Epitope mapping. Single-spot, 96-well standard plates (MSD) were coated overnight with 5 µl per well of 10 µg/ml DLL4 (R&D systems) in PBS with 0.03% Triton X-100. Control wells were left uncoated as blank. The next day, a 150 µl aliquot of 3% BSA in TBST was added to each well and allowed to incubate for 60 min at 20 °C to block the plate. After washing twice with 150 µl TBST and tap drying, 50 µl aliquots of 100 nM Ru-labeled M0008 plus a serial dilution of either M0022 or M0031, in duplicates, were added. After incubating the plate at 20 °C with shaking for 1 h, ECL was measured using a Sector Imager 2400. After subtracting the signals from the blank wells without DLL4, percent Ru-M0008 binding was calculated by dividing the ECL signal to the averaged signal with only Ru-labeled M0008.

Alanine-scanning mutagenesis and NNK mutagenesis. Oligos used for alanine-scanning mutagenesis were synthesized by Integrated DNA Technologies (IDT). The mutagenesis was carried out using standard overlapping PCR procedures. NNK mutagenesis by overlapping PCR was carried out similarly to the alanine scanning mutagenesis, except the target codon is replaced with NNK in the forward primer, and MNN in the reverse primer. After transformation of the ligation product in DH5α and plating, individual colonies were picked into 96-well blocks containing 1.5 ml of Terrific Broth (EMD) supplemented with 50 µg/ml kanamycin and 0.4% glucose per well, and grown at 37 °C overnight for isolating the plasmid of each mutation. DNA sequencing was used to identify the exact substitution of G100 in each well.

Cassette mutagenesis. We designed a straightforward cloning strategy to carry out cassette mutagenesis using Type II restriction enzymes such as BsaI. First, internal BsaI sites (if any) encoded by the plasmid were removed using the Quick Change Mutagenesis Kit (Stratagene). Depending on the CDR to be mutated, a vector was made to incorporate a BsaI site at the beginning and at the end of the CDR using overlapping PCR. The vector was then digested with BsaI and gel purified. A set of short forward and reverse primers carrying the desired mutation in the CDR were synthesized. When annealed, they formed compatible ends to the digested vector. The primer sets were mixed in TE ((tris[hydroxymethyl]-aminomethane), ethylenediaminetetraacetic acid) at 1 µM, heated at 95 °C for 2 min and slowly cooled down to 24 °C. One microliter of the annealed primers was ligated with 2 ng of the BsaI digested vector and transformed into DH5α cells. As long as the mutations were within the same CDR, the same vector was used for incorporating any mutations by ligation with short primer sets.

Enzyme-linked immunosorbent assay (ELISA) titration of anti-DLL4 Fabs. Nunc Maxisorp 384-well plates were coated with 10 µl per well of 0.5 µg/ml recombinant human DLL4 extracellular domain overnight at 4 °C. After blocking the plate with 1% BSA in TBST, a 20 µl aliquot of each serial dilution was added, in triplicate, to each well and the plate was incubated for 1 h at 24 °C followed by washing 2 times with 100 µl TBST. Depending on the light chain (either κ or λ), 20 µl of the corresponding goat anti-human kappa horseradish

peroxidase (HRP) conjugated polyclonal antibody (Sigma-Aldrich) or goat anti-human lambda HRP conjugated polyclonal antibody (Sigma-Aldrich) diluted 1:1,000 in 1% BSA TBST was added to each well and the plate was incubated for 1 h at 24 °C followed by washing 4× with 100 µl TBST. Finally, 25 µl TMB one-component reagent (BioFx) was added and allowed to develop for 1 to 10 min at 24 °C. The reaction was immediately stopped by the addition of 25 µl 0.5 M H_2S0_4 and the absorbance at 450 nm was measured on a plate reader (Molecular Devices).

K_d measurement by SPR. Binding studies were outsourced to Biosensor Tools. They were run on a ProteOn system using a GLM sensor chip in 10 mM HEPES (pH 7.4), 150 mM NaCl, 0.01% tween-20 and 0.1 mg/ml BSA at 25 °C. Each antigen was immobilized using amine coupling at three different surface densities. The Fabs were each tested at 1 µM as the highest concentration in a threefold dilution series. The response data from each surface were globally fit to determine the binding constants presented on each plot and averaged for the final report.

IgG cloning, expression and purification. Sequences encoding heavy and light chains were cloned separately into the pFUSE family of vectors (InvivoGen). To produce IgG, the heavy and light chain plasmids were co-transfected into 293FS cells (Invitrogen) using 293fectin (Invitrogen) per manufacturer's instructions. Cells growing in serum-free 293Freestyle medium (Invitrogen) were transfected at 1×10^6 cells/ml in a 50 ml spinner flask. Cell culture media was harvested 3 and 6 d after transfection and pooled together for purification on Protein-G Sepharose (GE Healthcare). IgG elution fractions were pooled and dialyzed into PBS.

DLL4 extracellular domain and DLL4 truncations preparation. Human DLL4 cDNA (Open Biosystems) was used as the template for PCR amplification of the full extracellular domain of DLL4 (aa 1–524), and several extracellular domain truncations: pre-DSL (aa 1–172), DSL (aa 1–217), EGF1 (aa 1–251), EGF2 (aa 1–286), EGF4 (aa 1–360) and EGF7 (aa 1–476). A myc tag and a 6-His tag were appended to the C termini of these constructs. The PCR products were cloned between the NheI and NotI sites of pcDNA5/FRT vector (Invitrogen) and transfected into the Flp-In CHO Cell Line (Invitrogen) according to the Flp-In System protocol. Transfected cells were selected with 400 µg/ml hygromycin after 2 d. After colony picking, cell lines were maintained at 37 °C with hygromycin selection. Expression media samples were collected after 7 d. One ml aliquots were batch bound with 50 µl of Talon Resin (CloneTech) for 30 min. Samples were washed, boiled with loading dye ± DTT, and resolved on a 4–12% Bis-Tris Gel (Invitrogen). Protein bands were transferred to PVDF membrane and probed with either 0.5 µg/ml anti-c-myc mAb (Genscript) to confirm protein secretion, or 20 nM M0026 or M0035 for epitope mapping. For detection goat anti-mouse HRP, anti-human kappa HRP, or anti-human lambda HRP (1,000-fold dilution) were used, respectively.

CHO-DLL4 binding and inhibition of DLL4-NOTCH1 interaction using flow cytometry. Full-length human DLL4 gene was digested out from the OpenBiosystems vector and ligated directly into pCDNA5/FRT between NheI and NotI sites. Transfection and colony selection were as described above.

CHO cells stably expressing full-length DLL4 or control CHO cells were detached from plates using Accutase (eBiosciences). Cells were washed in 2% BSA/PBS and incubated with 10–50 nM Fab in 2% BSA/PBS for 30 min. Phycoerythrin-labeled anti-human kappa (Invitrogen) for M0026 or phycoerythrin-labeled anti-human lambda (Invitrogen) for M0035 at a dilution of 1:30 were added to cells an incubated for 10 min. Cells were then washed in 2% BSA/PBS and analyzed by flow cytometry on a FACSAria (Becton Dickenson).

To test Fab inhibition of the NOTCH1-DLL4 interaction, cells were treated with 250 nM biotinylated NOTCH1-Fc and 0 to 50 nM Fab (either M0026 or M0035) for 30 min in 2% BSA/PBS. Phycoerythrin-labeled streptavidin (Pierce-Thermo Scientific) was then added to a final dilution of 1:5 and then incubated for 10 min. Cells were then washed in 2% BSA/PBS and analyzed by flow cytometry on a FACSAria.

Inhibition of NOTCH1 signal transduction. A NOTCH1 reporter construct (p6 × CBF) was made by inserting six CBF NOTCH-response elements (bold) into pGL4.26 (Promega): GGTACCTGAGCTCGCTAGCGATCTGGTGTAAACACGCC**GTGGGAA**AAAATTTATGGATCTGGTGTAAACACGCC**GTGGGAA**AAAATTTATGGAGCTCGCTAGCGATCTGGTGTAAACACGCC**GTGGGAA**AAAATTTATGGATCTGGTGTAAACACGCC**GTGGGAA**AAAATTTATGCTCGAGGATCTGGTGTAAACACGCC**GTGGGAA**AAAATTTATGGATCTGGTGTAAACACGCC**GTGGGAA**AAAATTTATGAAGCTT. The reporter plasmid was transfected into T98G glioma cells (ATCC), which express endogenous NOTCH1. Stable integrants were selected with 200 µg/ml Hygromycin B (Invitrogen), yielding a T98G NOTCH1 reporter cell line that induced Firefly luciferase expression upon NOTCH1 activation. CHO cells expressing DLL4 or control CHO cells were propagated in F12 media (Invitrogen) supplemented with 10% FBS and P/S/G. Separately, T98G NOTCH1 reporter cells (2×10^5 cells/well) in EMEM with 10% FBS and P/S/G were plated onto 96-well tissue culture plates. The next day, media was removed from the T98G cells and replaced with 100 µl CHO-DLL4 or control CHO cells (1×10^5 cells/well) in serum free F12 media supplemented with P/S/G. Inhibitory Fabs (M0026 and M0035) and their corresponding IgGs, and control Fabs (F1001) were added at 100, 20, 4 and 0.8 nM. After 24 h, luciferase-reporter expression was measured with Bright-Glo luciferase assay reagent (Promega). Luminescence was read using a Wallac Victor II model 1420 plate reader. Each condition was performed in quadruplicate. CHO cells (not expressing DLL4) were never seen to activate NOTCH1 reporter alone or in combination with any antibody (**Fig. 5e** and data not shown).

doi:10.1038/nbt.1694